Journal of Sound and Vibration (1997) **206**(5), 641–661

GENERAL PLANAR DYNAMICS OF A SLIDING FLEXIBLE LINK

B. O. Al-Bedoor and Y. A. Khulief

Department of Mechanical Engineering, King Fahd University of Petroleum and Minerals, KFUPM Box 841, *Dhahran* 31261, *Saudi Arabia*

(*Received* 18 *March* 1996, *and in final form* 30 *May* 1997)

A finite element dynamic model of a sliding link through a prismatic joint where the prismatic joint hub is executing general planar motion is formulated. In contrast to previously reported formulations, a finite element mesh with a fixed number of elements is used, where the element length is constant. The time-dependent boundary conditions manifested by the prismatic joint constraints are considered. A transition element with variable stiffness is introduced at the interface with the joint hub. In this finite element formulation, all the inertia coupling terms between the beam reference motions and the local elastic deformations are considered. In addition, the model accounts for the dynamics of the end mass as well as the associated coupling effects. Numerical simulations and comparisons with results obtained by other methods are presented to demonstrate the validity and accuracy of the model.

1. INTRODUCTION

The problem of modelling the dynamics of flexible beams with prismatic joints has attracted the attention of investigators in several areas of engineering applications. Examples of such applications are robotic manipulators, telescopic members of loading vehicles, and deployable space structures, in addition to other applications such as magnetic tape drives, printing machines, travelling cables and bandsaws. Flexible members with prismatic joints are known to produce considerable mathematical difficulty in the dynamic modelling of such systems. The problem becomes even more difficult if the beam is translating through a prismatic joint which is executing general planar motion. It has become evident that a reliable dynamic model for a translating and rotating beam that accounts for the interaction between rigid and flexible body motions is highly demanded. Such a dynamic model is crucial to the design, performance evaluation, and control of light-weight, high-speed, and high-precision applications.

The vibrational characteristics of a translating beam were first studied by Mote [1] in his work on band saws. In reference [1], the dependence of the natural frequencies on the velocity and initial tension in the band saw was reported. Other investigations were initiated to address the problem of modelling the dynamics of axially moving beams and links [2–5]. Space applications involving spacecraft with deployable appendages posed another area of interest where the dynamics of axially moving beams has been investigated [6–9]. Several other investigations [10–14] were directed to the study of the dynamic stability of moving bands and belts.

In all of the above mentioned investigations, only the translational motion of an elastic beam with prismatic joint was considered. Chalhoub and Ulsoy [15] investigated the effect of the structural flexibility on the control of a robotic arm with one prismatic and two

0022–460X/97/400641 + 21 $25.00/0/sv971129

revolute joints. The equations were derived by using the Lagrangian approach in conjunction with the assumed displacement approximation. Their model, however, did not account for the inertia coupling between the rigid body motion and the elastic deformations. Wang and Wei [16], proposed a feedback control law to minimize the vibrations of a flexible robot arm with revolute and prismatic joints. They utilized their earlier model [5] in addition to a prescribed rotational motion. Consequently, the effect of the elastic motion on the reference rotational motion did not appear in their equations. Krishnamurthy [17], extended the work of reference [16] by incorporating the dynamics of the beam tail. The choice of the body axes, however, resulted in a dynamic model wherein the inertia coupling between the translational motion and the elastic deformations was ignored. That is, if one eliminates the rotational degree of freedom from the equations of motion, the model of reference [17] is rendered uncoupled. Yuh and Young [18] developed a dynamic model of an axially moving and rotating beam, wherein the motion is confined to the horizontal plane. Newton's approach was employed in developing the equation of motion in the form of one partial differential equation. Using the assumed modes technique, they obtained a system of linear differential equations with time varying coefficients. It was found that the effect of the Coriolis acceleration on the elastic deformations was partially considered in their equation of motion. Following the same methodology of reference [4], Buffinton [19] modelled the dynamics of an elastic manipulator with a prismatic joint, wherein the prismatic joint was modelled as a two-part support. Recently, Al-Bedoor and Khulief [20] reported a general dynamic model for the translating and rotating beam that utilizes the assumed modes method, and accounts for all the interactions between rigid body motion and the elastic deformations.

Almost all the previously cited investigations have employed the assumed modes method to describe the motion of the continuum and to convert the dynamic model into a set of ordinary differential equations. Other investigators [21] modelled a translating and rotating beam by a set of elastically connected massless rigid links. These formulations were restricted to study the effects of the rigid body motion, in terms of the driving constraints, on the elastic deformations of a translating and rotating beam. Pan *et al*. [22] utilized the finite element method in modelling a flexible robot arm with prismatic and revolute joints. They discretized the beam by a fixed number of beam elements. The mesh size was allowed to change as a function of time in order to locate nodes at key points where the boundary conditions can be applied. The coupling effect due to the axial motion was ignored in their kinetic energy formulation and thus in the resulting equations of motion. Gordaninejad *et al*. [23] applied the same methodology to a robot arm made of composite materials. Kim and Gibson [24] used the finite element method to model a sliding flexible link. They considered the part of the link extending outside the prismatic joint to be composed of a fixed number of elements. The length of each element changes as the beam moves relative to the joint. The same methodology of employing a constant number of elements with variable length was also investigated by Downer and Park [25], and Stylianou and Tabarrok [26]. Vu-Quoc and Li [27] formulated the problem with time varying boundary conditions. They considered that the prismatic joint is moving with respect to the beam. The time varying problem defined over the interval $[0, L(t)]$ was converted to what they called "constant stretched co-ordinates" over the interval [0, 1]. The new hypothetical domain was then discretized by using a fixed number of elements with constant lengths since the domain [0, 1] is not changing with time. An available finite element code was used to simulate this problem with coefficient matrices changing at each time step. Post-processing, as they mentioned, was needed to convert the results back into the actual physical domain. It is noteworthy to mention here that those time varying matrices are equivalent to the methodology of using a finite element domain with changing element

lengths. The method of converting the domain into a fixed domain was used by Al-Bedoor and Khulief [28] in reporting an approximate analytical solution of beam vibration during axial motion. Recently, Al-Bedoor and Khulief [29] reported a finite element dynamic model of a sliding and rotating flexible link using fixed number of elements with constant lengths.

The current status of the reported approaches and methodologies indicate the following. (a) The majority of the published studies were directed to modelling the dynamics of only the translational motion of a sliding beam. (b) The investigations that addressed both the translational and rotational motions were restricted to the case where the prismatic joint hub rotates about a fixed axis. (c) Most of the reported finite element models have employed a changeable finite element mesh by considering the element length as a function of time. As a result of adopting a changeable finite element mesh and thus separating the mathematical model from the physical problem, some of these models have fallen short of accounting for all the dynamic coupling terms. In addition to the numerical difficulties associated with the changeable finite element mesh, one must recognize another potential problem of preserving the continuity of the nodal displacements and velocities when interfacing the old nodes with the new ones.

In this paper, a general dynamic model for a sliding flexible link through a prismatic joint where the prismatic joint hub is executing general planar motion is developed. The Lagrangian approach in conjunction with the finite element technique is employed. The finite element formulation adopts a fixed number of elements, where each finite element has a constant length. Consequently, the formulation results in an unchangeable finite element mesh. This feature is essential for control applications where point-sensors and point-actuators are placed at fixed nodal points. In this formulation, the prismatic joint hub is treated as rigid, and the nodal points housed inside it have zero displacements and zero slopes. The time dependent boundary conditions as manifested by the prismatic joint constraints are accounted for by imposing zero elastic displacement and velocity for each node housed inside the hub of the prismatic joint. The element which has one of its nodes housed inside the hub of the prismatic joint while the other node is outside the joint is called the transition element. The transition element is neither a totally free element like those located outside the hub of the prismatic joint nor a totally rigid element like those completely housed inside the hub of the prismatic joint. To allow smooth transfer from the case of flexible element to the case of rigid element and *vice versa*, the stiffness of the transition element is changed as function of its free hanging length which in turn is a function of time. Furthermore, this methodology has the advantage of using a minimum number of elements without loss of accuracy. The model take account of all the rigid body motions and the relative elastic deformations in their coupled format. As a result of this formulation, studying the effects of rigid body motions on the elastic deformations and the other way around are made possible. Numerical simulations and comparisons are presented to demonstrate the validity and the accuracy of the model.

2. THE ELASTODYNAMIC FORMULATION

A beam with a prismatic joint hub in general planar motion, shown in Figure 1, is considered with the following features and assumptions. (1) The prismatic joint hub is rigid and the motion of the beam inside the prismatic joint is frictionless. (2) The beam is inextensible and Euler–Bernoulli beam theory is adopted. (3) The gravitational potential energy due to the elastic deformations is neglected compared to the overall reference motion. (4) A tip mass is considered to be concentrated at the free end of the beam. The rotary inertia of the tip mass is neglected.

2.1. GENERALIZED CO-ORDINATES AND VELOCITIES

In this formulation, the Lagrangian approach is employed. Therefore, one needs to evaluate both the kinetic and potential energy expressions. To this end, one must define the global position of an arbitrary point on the beam. Let XY represent the inertial frame, and the co-ordinate system x^1y^1 be fixed to the prismatic joint hub. The x^2y^2 co-ordinate system is attached to the beam and is moving with it, but remains parallel to the x^1-, y^1-axes. The beam is described by using n finite elements. A typical element i is considered to have two nodes: namely, i and $i+1$. The co-ordinate system xy is the ith element co-ordinate system defined with respect to the undeformed state. The global position of an arbitrary point p on the ith element of the beam thus can be written as

$$R_p = R_{o1} + Ar_p, \tag{1}$$

where r_p is the position vector of point p in the x^1y^1 co-ordinate system, A is the rotational transformation matrix from the x^1y^1 co-ordinate system to the XY inertial reference frame and R_{o1} in the position of the x^1y^1 co-ordinate system in the inertial reference frame and can be expressed as

$$R_{o1} = XI + YJ. \tag{2}$$

(A list of nomenclature is given in the Appendix.)

The position vector of point p in the x^1y^1 co-ordinate system can be written in the form

$$r_p = (x^1_{o2} + x^2_i + x_p)i_1 + uj_1, \tag{3}$$

but, from Figure 1, one can define

$$S_i = x^1_{o2} + x^2_i, \tag{4}$$

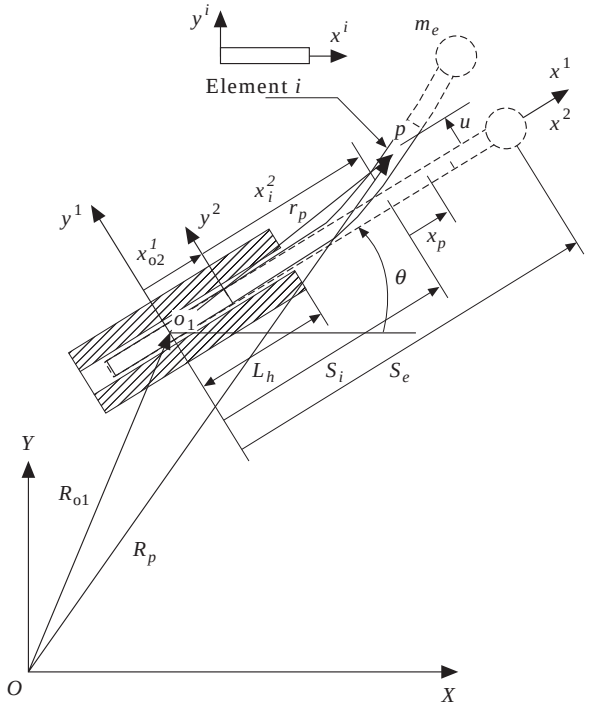

Figure 1. The co-ordinate system of a sliding link.

where S_i defines the axial position of node i in the co-ordinate system x^1y^1 and is chosen to represent the translational degree of freedom of the system. Upon substituting equation (4) into equation (3), the position vector of point p in the body co-ordinate system x^1y^1 becomes

$$r_p = (S_i + x_p)i_1 + uj_1, \tag{5}$$

where u is the transverse elastic displacement of the beam at point p measured relative to the x^1y^1 co-ordinate system. In order to formulate the kinetic energy expression, the velocity vector can be written as

$$\dot{R}_p = \dot{R}_{o1} + A\dot{r}_p + \dot{\theta}(A_\theta)r_p, \tag{6}$$

where $A_\theta = \partial A/\partial\theta$, and $(\dot{})$ denotes differentiation with respect to time.

Upon differentiation of equation (5) and carrying out some algebraic manipulation of equation (6), the velocity vector of point p can be expressed as

$$\dot{R}_p = \begin{Bmatrix} \dot{X} - \sin\theta[\dot{u} + \dot{S}u' + \dot{\theta}(S_i + x_p)] + \cos\theta[\dot{S} - \dot{\theta}u] \\ \dot{Y} + \sin\theta[\dot{S} - \dot{\theta}u] + \cos\theta[\dot{u} + \dot{S}u' + \dot{\theta}(S_i + x_p)] \end{Bmatrix}, \tag{7}$$

where the subscript i in the velocity term $\dot{S}_i$ has been dropped for simplicity of notation, and $(')$ denotes differentiation with respect to x.

2.2. THE KINETIC ENERGY EXPRESSIONS FOR THE BEAM ELEMENT

The kinetic energy of a typical element i with mass per unit length ρ and length l can be written in the form

$$U_i = \tfrac{1}{2}\int_0^l \rho \dot{R}_p^{\mathrm{T}} \dot{R}_p \, \mathrm{d}x. \tag{8}$$

Substituting equation (7) into equation (8) yields

$$\begin{aligned} U_i = {} & \tfrac{1}{2}\int_0^l \rho\{[\dot{u} + \dot{S}u' + \dot{\theta}(S_i + x_p)]^2 + [\dot{S} - \dot{\theta}u]^2\} \, \mathrm{d}x \\ & + \tfrac{1}{2}\int_0^l \rho\{\dot{X}^2 + \dot{Y}^2 + 2[\dot{u} + \dot{S}u' + \dot{\theta}(S_i + x_p)]\dot{Y}\cos\theta\} \, \mathrm{d}x \\ & + \tfrac{1}{2}\int_0^l \rho\{-2[\dot{u} + \dot{S}u' + \dot{\theta}(S_i + x_p)]\dot{X}\sin\theta\} \, \mathrm{d}x \\ & + \tfrac{1}{2}\int_0^l \rho\{2[\dot{S} - \dot{\theta}u]\dot{X}\cos\theta + 2[\dot{S} - \dot{\theta}u]\dot{Y}\sin\theta\} \, \mathrm{d}x. \end{aligned} \tag{9}$$

2.3. THE POTENTIAL ENERGY EXPRESSIONS FOR THE BEAM ELEMENT

The potential energy of the system is constituted of the elastic strain energy, the gravitational potential energy and the potential energy of the axial shortening due to the

transverse deformations and the axial inertial forces. The elastic strain energy stored in element i which has a flexural rigidity EI can be written in the form

$$V_{si} = \tfrac{1}{2}\int_0^l EI(x)\left[\frac{\partial^2 u}{\partial x^2}\right]^2 \mathrm{d}x. \tag{10}$$

The gravitational potential energy due to the reference motion can be expressed as

$$V_{gi} = \rho g Y l + \rho g S_i l \sin\theta + \rho g (l^2/2)\sin\theta. \tag{11}$$

For evaluating the axial potential energy of shortening, the amount of shortening can be represented by

$$\mathrm{d}\delta \cong -\tfrac{1}{2}(\partial u/\partial x)^2\,\mathrm{d}x, \tag{12}$$

while the axial inertial force that results from the reference motion of element i can be written in the following form:

$$F_p = \int_x^l \rho[\ddot{S} + \ddot{X}\cos\theta + \ddot{Y}\sin\theta - \dot{\theta}^2(S_i + x)]\,\mathrm{d}x$$

$$+ \sum_{j=i+1}^{n} \rho_j l_j\left[\ddot{S} + \ddot{X}\cos\theta + \ddot{Y}\sin\theta - \left(S_j + \frac{l_j}{2}\right)\dot{\theta}^2\right]. \tag{13}$$

The element axial shortening potential energy can then be expressed as

$$V_{ai} = \int_0^l F_p\,\mathrm{d}\delta. \tag{14}$$

Evaluating the integral of equation (13) and substituting the result together with equation (12) into equation (14), one obtains the following expression for the axial shortening potential energy:

$$V_{ai} = \tfrac{1}{2}\int_0^l \left\{\rho[(S_i\dot{\theta}^2 - \ddot{S} - \ddot{X}\cos\theta - \ddot{Y}\sin\theta)(l - x) + \tfrac{1}{2}\dot{\theta}^2(l^2 - x^2)]\left(\frac{\partial u}{\partial x}\right)^2\right\}\mathrm{d}x$$

$$-\tfrac{1}{2}(\ddot{\mathrm{S}} + \ddot{\mathrm{X}}\cos\theta + \ddot{Y}\sin\theta)\sum_{j=i+1}^{n}\rho_j l_j\int_0^l\left(\frac{\partial u}{\partial x}\right)^2\mathrm{d}x$$

$$+\frac{\dot{\theta}^2}{2}\sum_{j=i+1}^{n}\left(S_j + \frac{l_j}{2}\right)\rho_j l_j\int_0^l\left(\frac{\partial u}{\partial x}\right)^2\mathrm{d}x. \tag{15}$$

2.4. THE PRISMATIC JOINT HUB CONTRIBUTION

The hub of the prismatic joint shown in Figure 1 is considered to be rigid and is executing a general planar motion. Its contribution to the system's kinetic energy can be represented by

$$U_h = \tfrac{1}{2}J_h\dot{\theta}^2 + \tfrac{1}{2}m_h\dot{X}^2 + \tfrac{1}{2}m_h\dot{Y}^2, \tag{16}$$

where m_h and J_h are the mass and the mass moment of inertia of the prismatic joint hub respectively. The hub of the prismatic joint contributes also to the gravitational potential energy of the system, by the term

$$V_h = m_h g Y. \tag{17}$$

2.5. THE END MASS CONTRIBUTION

The end mass contributes to the dynamics of the system through its kinetic energy, gravitational potential energy as well as its axial shortening potential energy. The end mass is assumed to be attached to the tip node of the beam. By using an analysis similar to that leading to equation (7), one can write the velocity vector of the end mass as

$$\dot{R}_e = \begin{Bmatrix} \dot{X} - \sin\theta[\dot{u}_e + \dot{S}u_e' + \dot{\theta}S_e] + \cos\theta[\dot{S} - \dot{\theta}u_e] \\ \dot{Y} + \sin\theta[\dot{S} - \dot{\theta}u_e] + \cos\theta[\dot{u}_e + \dot{S}u_e' + \dot{\theta}S_e] \end{Bmatrix}. \tag{18}$$

The kinetic energy of the end mass can then be expressed as

$$U_e = \tfrac{1}{2} m_e \dot{R}_e^{\mathrm{T}} \dot{R}_e. \tag{19}$$

Substituting equation (18) into equation (19) yields the end mass kinetic energy as

$$\begin{aligned} U_e = \tfrac{1}{2} m_e [&\dot{X}^2 + \dot{Y}^2 + \dot{S}^2 + \dot{\theta}^2 u_e^2 + \dot{u}_e^2 + \dot{S}^2 u_e'^2 + \dot{\theta}^2 S_e^2 - 2\dot{S}\dot{\theta}u_e \\ &+ 2\dot{S}\dot{u}_e u_e' + 2\dot{\theta}S_e\dot{u}_e + 2\dot{\theta}S_e\dot{S}u_e' + 2\dot{X}\cos\theta\dot{S} - 2\dot{X}\dot{\theta}u_e\cos\theta + 2\dot{Y}\dot{S}\sin\theta - 2\dot{Y}\dot{\theta}u_e\sin\theta \\ &+ 2\dot{Y}\dot{u}_e\cos\theta + 2\dot{Y}\dot{S}u_e'\cos\theta + 2\dot{Y}\dot{\theta}S_e\cos\theta \\ &- 2\dot{X}\dot{u}_e\sin\theta - 2\dot{X}\dot{S}u_e'\sin\theta - 2\dot{X}\dot{\theta}S_e\sin\theta]. \end{aligned} \tag{20}$$

The gravitational potential energy of the end mass can be expressed as

$$V_{ge} = m_e g Y + m_e g S_e \sin\theta. \tag{21}$$

By following the previously stated methodology, the axial shortening potential energy can be approximated to the form

$$V_{ae} = \tfrac{1}{2} m_e (S_e\dot{\theta}^2 - \ddot{S} - \ddot{X}\cos\theta - \ddot{Y}\sin\theta)(S_e - L_h)(\partial u_e/\partial x)^2. \tag{22}$$

2.6. ENERGY EXPRESSIONS FOR THE WHOLE SYSTEM

The system kinetic and potential energy expressions can be expressed, respectively, as

$$U = \sum_{i=1}^{n} U_i + U_e + U_h \tag{23}$$

and

$$V = \sum_{i=1}^{n} (V_i + V_{gi} + V_{ai}) + V_{ge} + V_{ae} + V_{gh}, \tag{24}$$

where n is the number of elements comprising the beam.

3. THE FINITE ELEMENT DISCRETIZATION

The finite element method will be utilized to discretize the elastic deformations. In the finite element method, the deformations are represented in terms of the nodal degrees of freedom. This can be expressed as

$$u(x, t) = [N(x)]\{q(t)\}, \tag{25}$$

where $[N]$ is a raw matrix of the shape functions which are spatially dependent, and $\{q\}$ is the vector of nodal degrees of freedom which are time dependent.

3.1. ENERGY EXPRESSIONS FOR THE FINITE BEAM ELEMENT

By utilizing the time and spatial derivatives of the elastic deformation $u(x, t)$, the kinetic energy of the element i can be written in the form

$$\begin{aligned}
U_i = {} & \tfrac{1}{2}\rho l\dot{S}^2 + \tfrac{1}{2}\rho l\dot{\theta}^2(S_i^2 + l^2/3 + S_i l) + \tfrac{1}{2}\rho l\dot{X}^2 + \tfrac{1}{2}\rho l\dot{Y}^2 + \rho l\dot{\theta}S_i\dot{Y}\cos\theta \\
& - \rho l\dot{\theta}S_i\dot{X}\sin\theta + \rho l\dot{S}\dot{X}\cos\theta + \rho l\dot{S}\dot{Y}\sin\theta + \tfrac{1}{2}l^2\rho\dot{\theta}\dot{Y}\cos\theta - \tfrac{1}{2}\rho l^2\dot{\theta}\dot{X}\sin\theta \\
& + \tfrac{1}{2}\int_0^l \rho\{\dot{q}\}^{\mathrm{T}}[N]^{\mathrm{T}}[N]\{\dot{q}\}\,\mathrm{d}x + \tfrac{1}{2}\dot{\theta}^2\{q\}^{\mathrm{T}}\int_0^l \rho[N]^{\mathrm{T}}[N]\,\mathrm{d}x\{q\} \\
& + \tfrac{1}{2}\dot{S}^2\int_0^l \rho\{q\}^{\mathrm{T}}[N']^{\mathrm{T}}[N']\{q\}\,\mathrm{d}x + \dot{S}\int_0^l \rho\{q\}^{\mathrm{T}}[N']^{\mathrm{T}}[N]\{\dot{q}\}\,\mathrm{d}x \\
& - \dot{\theta}\dot{S}\int_0^l \rho[N]\,\mathrm{d}x\{q\} + S_i\dot{\theta}\int_0^l \rho[N]\,\mathrm{d}x\{\dot{q}\} + \dot{\theta}\int_0^l \rho x[N]\,\mathrm{d}x\{\dot{q}\} \\
& + \dot{\theta}\dot{S}S_i\int_0^l \rho[N']\,\mathrm{d}x\{q\} + \dot{\theta}\dot{S}\int_0^l \rho x[N']\,\mathrm{d}x\{q\} + \dot{Y}\cos\theta\int_0^l \rho[N]\,\mathrm{d}x\{\dot{q}\} \\
& + \dot{Y}\dot{S}\cos\theta\int_0^l \rho[N']\,\mathrm{d}x\{q\} - \dot{X}\sin\theta\int_0^l \rho[N]\,\mathrm{d}x\{\dot{q}\} - \dot{X}\dot{S}\sin\theta\int_0^l \rho[N']\,\mathrm{d}x\{q\} \\
& - \dot{\theta}\dot{X}\cos\theta\int_0^l \rho[N]\,\mathrm{d}x\{q\} - \dot{\theta}\dot{Y}\sin\theta\int_0^l \rho[N]\,\mathrm{d}x\{q\},
\end{aligned} \tag{26}$$

and the bending strain energy of element i can be written as

$$V_{si} = \tfrac{1}{2}\int_0^l EI(x)[\{q\}^{\mathrm{T}}[N'']^{\mathrm{T}}[N'']\{q\}]\,\mathrm{d}x, \tag{27}$$

while the axial shortening potential energy of element i can be written in the form

$$V_{ai} = \tfrac{1}{2}(S_i\dot{\theta}^2 - \ddot{S} - \ddot{X}\cos\theta - \ddot{Y}\sin\theta)\{q\}^{\mathrm{T}} \int_0^l \rho[N']^{\mathrm{T}}[N'](l-x)\,\mathrm{d}x\{q\}$$

$$+\tfrac{1}{4}\dot{\theta}^2\{q\}^{\mathrm{T}} \int_0^l \rho[N']^{\mathrm{T}}[N'](l^2 - x^2)\,\mathrm{d}x\{q\}$$

$$+\tfrac{1}{2}\sum_{j=i+1}^{n}\left(S_j + \frac{l_j}{2}\right)\rho_j l_j\dot{\theta}^2\{q\}^{\mathrm{T}} \int_0^l [N']^{\mathrm{T}}[N']\,\mathrm{d}x\{q\}$$

$$-\tfrac{1}{2}(\ddot{S} + \ddot{X}\cos\theta + \ddot{Y}\sin\theta)\sum_{j=i+1}^{n}\rho_j l_j\{q\}^{\mathrm{T}} \int_0^l [N']^{\mathrm{T}}[N']\{q\}. \tag{28}$$

3.2. EQUATIONS OF MOTION

The Lagrangian approach is employed in deriving the equations of motion at the element level. By utilizing the kinetic and potential energy expressions, equations (26–28) in the variational form of the Lagrange's equation, and performing the required differentiations and algebraic manipulations, the equations of motion at the element level can be written in the following compact form:

$$\begin{bmatrix} m_{XX} & m_{XY} & m_{X\theta} & m_{XS} & [m_{Xq}] \\ m_{YX} & m_{YY} & m_{Y\theta} & m_{YS} & [m_{Yq}] \\ m_{\theta X} & m_{\theta Y} & m_{\theta\theta} & m_{\theta S} & [m_{\theta q}] \\ m_{SX} & m_{SY} & m_{S\theta} & m_{SS} & [m_{Sq}] \\ [m_{qX}] & [m_{qY}] & [m_{q\theta}] & [m_{qS}] & [m_{qq}] \end{bmatrix} \begin{Bmatrix} \ddot{X} \\ \ddot{Y} \\ \ddot{\theta} \\ \ddot{S} \\ \{\ddot{q}\} \end{Bmatrix} + \dot{S} \begin{bmatrix} 0 & 0 & 0 & 0 & 0 \\ 0 & 0 & 0 & 0 & 0 \\ 0 & 0 & 0 & 0 & 0 \\ 0 & 0 & 0 & 0 & 0 \\ 0 & 0 & 0 & 0 & [G] \end{bmatrix}$$

$$\times \begin{Bmatrix} \dot{X} \\ \dot{Y} \\ \dot{\theta} \\ \dot{S} \\ \{\dot{q}\} \end{Bmatrix} + \begin{bmatrix} 0 & 0 & 0 & 0 & 0 \\ 0 & 0 & 0 & 0 & 0 \\ 0 & 0 & 0 & 0 & 0 \\ 0 & 0 & 0 & 0 & 0 \\ 0 & 0 & 0 & 0 & [k_{qq}] \end{bmatrix} \begin{Bmatrix} X \\ Y \\ \theta \\ S_i \\ \{q\} \end{Bmatrix}$$

$$+ \begin{Bmatrix} Q_X \\ Q_Y \\ Q_\theta \\ Q_S \\ \{Q_q\} \end{Bmatrix} = \begin{Bmatrix} F_X \\ F_Y \\ F_\theta \\ F_S \\ \{F_q\} \end{Bmatrix}, \tag{29}$$

where

$$m_{XX} = m_{YY} = \rho l + m_h, \qquad m_{XY} = 0, \tag{30}$$

$$m_{XS} = \rho l\cos\theta - \sin\theta[b]\{q\}, \qquad m_{YS} = \rho l\sin\theta + \cos\theta[b]\{q\}, \tag{31}$$

$$[m_{Xq}] = -\sin\theta[a], \qquad [m_{Yq}] = \cos\theta[a]; \qquad m_{\theta S} = [S_i[b] + [d] - [a]]\{q\},$$

$$[m_{\theta q}] = S_i[a] + [e], \tag{32, 33}$$

$$m_{SS} = \rho l + \{q\}^{\mathrm{T}}[B]\{q\}, \qquad [m_{Sq}] = \{q\}^{\mathrm{T}}[C]; \qquad [m_{qq}] = [M], \qquad [G] = [C]^{\mathrm{T}} - [C], \tag{34, 35}$$

$$m_{X\theta} = -[\rho l \sin\theta(S_i + \tfrac{1}{2}l) + \cos\theta[a]\{q\}], \qquad m_{Y\theta} = \rho l \cos\theta(S_i + \tfrac{1}{2}l) - \sin\theta[a]\{q\}, \tag{36, 37}$$

$$m_{\theta\theta} = J_h + \rho l(S_i^2 + l^2/3 + S_i l) + \{q\}^{\mathrm{T}}[[M] - S_i[k_{a1}] - \tfrac{1}{2}[k_{a2}]]\{q\}$$

$$- \sum_{j=i+1}^{n} \frac{\rho_j l_j}{\rho_i}\left(S_j + \frac{l_j}{2}\right)\{q\}^{\mathrm{T}}[B]\{q\}, \tag{38}$$

$$[k_{qq}] = [K] - \dot{S}^2[B] - \dot{\theta}^2\left([M] - S_i[k_{a1}] - \tfrac{1}{2}[k_{a2}] - \sum_{j=i+1}^{n} \frac{\rho_j l_j}{\rho_i}\left(S_j + \frac{l_j}{2}\right)[B]\right)$$

$$-(\ddot{S} + \ddot{X}\cos\theta + \ddot{Y}\sin\theta)\left[[k_{a1}] + \sum_{j=i+1}^{n} \frac{\rho_j l_j}{\rho_i}[B]\right], \tag{39}$$

$$Q_X = -\dot{S}\dot{\theta}(2\rho l \sin\theta + \cos\theta[b]\{q\}) - \dot{S}\sin\theta[b]\{\dot{q}\}$$

$$+\dot{\theta}^2(\sin\theta[a]\{q\} - \rho l(S_i + l/2)\cos\theta) - 2\dot{\theta}\cos\theta[a]\{\dot{q}\}, \tag{40}$$

$$Q_Y = \dot{S}\dot{\theta}(2\rho l\cos\theta - \sin\theta[b]\{q\}) + \dot{S}\cos\theta[b]\{\dot{q}\}$$

$$-\dot{\theta}^2(\cos\theta[a]\{q\} + \rho l(S_i + l/2)\sin\theta) - 2\dot{\theta}\sin\theta[a]\{\dot{q}\} + \rho g l + m_h g, \tag{41}$$

$$Q_\theta = \dot{S}\dot{\theta}\left[2\rho l(S_i + l/2) - \{q\}^{\mathrm{T}}\left([k_{a1}] + \sum_{j=i+1}^{n} \frac{\rho_j l_j}{\rho_i}[B]\right)\{q\}\right] + \dot{S}(S_i[b] + [d])\{\dot{q}\}$$

$$+\dot{S}^2[b]\{q\} + 2\dot{\theta}\{q\}^{\mathrm{T}}\left([M] - S_i[k_{a1}] - \tfrac{1}{2}[k_{a2}] - \sum_{j=i+1}^{n} \frac{\rho_j l_j}{\rho_i}[B]\right)\{\dot{q}\}$$

$$+\dot{S}\dot{Y}\sin\theta[b]\{q\} + \dot{S}\dot{X}\cos\theta[b]\{q\} + \rho g l\cos\theta(S_i + l/2)$$

$$+\tfrac{1}{2}(\ddot{X}\sin\theta - \ddot{Y}\cos\theta)\{q\}^{\mathrm{T}}[k_{a1}]\{q\} + \tfrac{1}{2}(\ddot{X}\sin\theta - \ddot{Y}\cos\theta)\sum_{j=i+1}^{n} \frac{\rho_j l_j}{\rho_i}\{q\}^{\mathrm{T}}[B]\{q\}, \tag{42}$$

$$Q_S = \{\dot{q}\}^{\mathrm{T}}[C]\{\dot{q}\} + 2\dot{S}\{q\}^{\mathrm{T}}[B]\{\dot{q}\} + \dot{\theta}([d] + S_i[b] - 2[a])\{\dot{q}\}$$

$$-\rho l\dot{\theta}^2[S_i + l/2] + \rho g l\sin\theta + \tfrac{1}{2}\dot{\theta}^2\{q\}^{\mathrm{T}}[k_{a1}]\{q\} - \dot{Y}\dot{\theta}\sin\theta[b]\{q\}$$

$$-\dot{X}\dot{\theta}\cos\theta[b]\{q\} + \dot{Y}\cos\theta[b]\{\dot{q}\} - \dot{X}\sin\theta[b]\{\dot{q}\}, \tag{43}$$

$$\{Q_q\} = \dot{S}\dot{\theta}[2[a] - S_i[b] - [d]]^{\mathrm{T}} + \dot{S}\dot{X}\sin\theta[b]^{\mathrm{T}} - \dot{S}\dot{Y}\cos\theta[b]^{\mathrm{T}}. \tag{44}$$

The element coefficient matrices and vectors are

$$[M] = \int_0^l \rho[N]^{\mathrm{T}}[N]\,\mathrm{d}x, \qquad [K] = \int_0^l EI(x)[N'']^{\mathrm{T}}[N'']\,\mathrm{d}x, \tag{45}$$

$$[B] = \int_0^l \rho[N']^{\mathrm{T}}[N']\,\mathrm{d}x, \qquad [C] = \int_0^l \rho[N']^{\mathrm{T}}[N]\,\mathrm{d}x, \tag{46}$$

$$[k_{a1}] = \int_0^l \rho(l-x)[N']^{\mathrm{T}}[N']\,\mathrm{d}x, \qquad [k_{a2}] = \int_0^l \rho(l^2-x^2)[N']^{\mathrm{T}}[N']\,\mathrm{d}x, \tag{47}$$

$$[a] = \int_0^l \rho[N]\,\mathrm{d}x, \qquad [b] = \int_0^l \rho[N']\,\mathrm{d}x; \qquad [d] = \int_0^l \rho x[N']\,\mathrm{d}x, \qquad [e] = \int_0^l \rho x[N]\,\mathrm{d}x. \tag{48, 49}$$

In equation (29), one can recognize the non-linear inertia coupling between the rigid body motions and the elastic deformations. The entries m_{XX} and m_{YY} are the assembly translational inertia, the entry $m_{\theta\theta}$ is the rotational inertia of the system, m_{SS} is the axial inertia of the system and $[m_{qq}]$ is the elastic mass matrix. The contribution of the elastic deformations to both the rotational and translational inertia terms m_{XX}, m_{YY}, $m_{\theta\theta}$ and m_{SS} is recognized in equations (30–35). The entries $m_{X\theta}$, m_{XS}, m_{Xq}, $m_{Y\theta}$, m_{YS}, m_{Yq}, $m_{\theta S}$, $m_{\theta q}$ and m_{Sq} represent the non-linear inertia coupling between the beam reference motions and the local elastic deformations. The matrix $[G]$ is the gyrosopic matrix, and $[k_{qq}]$ is the generalized stiffness matrix. The entries Q_X, Q_Y, Q_θ, Q_S and $\{Q_q\}$ of the non-linear vector represent inertia forces that result from the quadratic velocity terms, Coriolis accelerations, as well as the gravitational effects. The right side of equation (29) represents the vector of external forces and moments.

The contribution of the end mass to the dynamics of the system can be included by applying Lagrange's equation to the energy expressions of the end mass, equations (20–22). The result after, differentiation and algebraic manipulation, can be represented in the matrix form

$$\begin{bmatrix} m^e_{XX} & m^e_{XY} & m^e_{X\theta} & m^e_{XS} & m^e_{Xq_e} \\ & m^e_{YY} & m^e_{Y\theta} & m^e_{YS} & m^e_{Yq_e} \\ & & m^e_{\theta\theta} & m^e_{\theta S} & m^e_{\theta q_e} \\ & \text{Symmetric} & & m^e_{SS} & m^e_{Sq_e} \\ & & & & m'_{q_e q_e} \end{bmatrix} \begin{Bmatrix} \ddot{X} \\ \ddot{Y} \\ \ddot{\theta} \\ \ddot{S} \\ \ddot{q}_e \end{Bmatrix} + \begin{Bmatrix} Q^e_X \\ Q^e_Y \\ Q^e_\theta \\ Q^e_S \\ Q^e_{q_e} \\ Q^e_{q'_e} \end{Bmatrix} = \begin{Bmatrix} 0 \\ 0 \\ 0 \\ 0 \\ 0 \end{Bmatrix}, \tag{50}$$

where

$$m^e_{XX} = m^e_{YY} = m_e, \qquad m^e_{XY} = 0, \tag{51}$$

$$m^e_{X\theta} = -m_e(q_e\cos\theta + S_e\sin\theta), \qquad m_{Y\theta} = m_e(S_e\cos\theta - q_e\sin\theta), \tag{52}$$

$$m^e_{XS} = m_e(\cos\theta - q'_e\sin\theta), \qquad m^e_{YS} = m_e(\sin\theta + q'_e\cos\theta), \tag{53}$$

$$m^e_{Xq_e} = -m_e\sin\theta, \qquad m^e_{Yq_e} = m_e\cos\theta, \tag{54}$$

$$m^e_{\theta\theta} = m_e[q_e^2 + S_e^2 - S_e(S_e - L_h)q_e'^2], \qquad m^e_{\theta S} = m_e(S_e q_e' - q_e), \tag{55}$$

$$m^e_{\theta q_e} = m_e S_e, \qquad m^e_{Sq_e} = m_e q_e'; \qquad m^e_{SS} = m_e(1 + q_e'^2), \qquad m^e_{qq} = m_e, \tag{56, 57}$$

$$\begin{aligned} Q^e_X = & -m_e\dot{S}\dot{\theta}(2\sin\theta + q_e'\cos\theta) + m_e\dot{\theta}^2(q_e\sin\theta - S_e\cos\theta) \\ & - 2m_e\dot{\theta}\dot{q}_e\cos\theta - m_e\dot{S}\dot{q}_e'\sin\theta, \end{aligned} \tag{58}$$

$$\begin{aligned} Q^e_Y = & m_e\dot{S}\dot{\theta}(2\cos\theta - q_e'\sin\theta) - m_e\dot{\theta}^2(q_e\cos\theta + S_e\sin\theta) \\ & - 2m_e\dot{\theta}\dot{q}_e\sin\theta + m_e\dot{S}\dot{q}_e'\cos\theta + m_e g, \end{aligned} \tag{59}$$

$$\begin{aligned} Q^e_\theta = & m_e\dot{S}\dot{\theta}[S_e - (2S_e - L_h)q_e'^2] + m_e\dot{S}^2 q_e' + m_e S_e\dot{S}\dot{q}_e' + 2m_e\dot{\theta}q_e\dot{q}_e - 2m_e S_e\dot{\theta}(S_e - L_h)q_e'\dot{q}_e' \\ & + m_e g S_e\cos\theta + m_e\dot{Y}\dot{S}q_e'\sin\theta + m_e\dot{X}\dot{S}q_e'\cos\theta \\ & + \tfrac{1}{2}m_e\ddot{X}\sin\theta(S_e - L_h)q_e'^2 - \tfrac{1}{2}m_e\ddot{Y}\cos\theta(S_e - L_h)q_e'^2, \end{aligned} \tag{60}$$

$$\begin{aligned} Q^e_S = & -2m_e\dot{\theta}\dot{q}_e + 2m_e\dot{S}q_e'\dot{q}_e' + m_e\dot{q}_e\dot{q}_e' + m_e\dot{\theta}S_e\dot{q}_e' - m_e S_e\dot{\theta}^2 + m_e g\sin\theta \\ & + \tfrac{1}{2}m_e\dot{\theta}^2(2S_e - L_h)q_e'^2 + m_e\dot{Y}\dot{q}_e'\cos\theta - m_e\dot{Y}\dot{\theta}q_e'\sin\theta - m_e\dot{X}\dot{q}_e'\sin\theta \\ & - m_e\dot{X}\dot{\theta}q_e'\cos\theta - \tfrac{1}{2}m_e\cos\theta\ddot{X}q_e'^2 - \tfrac{1}{2}m_e\sin\theta\ddot{Y}q_e'^2, \end{aligned} \tag{61}$$

$$Q^e_{q_e} = 2m_e\dot{S}\dot{\theta} + m_e\dot{S}\dot{q}_e' - m_e q_e\dot{\theta}^2, \tag{62}$$

$$\begin{aligned} Q^e_{q_e'} = & m_e[S_e\dot{\theta}^2 - \ddot{S} - \ddot{X}\cos\theta - \ddot{Y}\sin\theta](S_e - L_h)q_e' \\ & + m_e\dot{X}\dot{S}\sin\theta - m_e\dot{Y}\dot{S}\cos\theta - m_e S_e\dot{S}\dot{\theta} - m_e\dot{S}^2 q_e'. \end{aligned} \tag{63}$$

The entries of equation (50) are to be added to the other elements of the corresponding generalized matrices in the equations of motion of the whole system. One can recognize the non-linear coupling terms due to the effect of the end mass, as given by equation (50). It is noteworthy to mention that, as a result of the consistent inclusion of the end mass dynamics from the start of the formulation the above coupling terms are obtained. Such terms were suppressed in the previously published formulations where the end mass contribution was simply added to the mass matrix at locations of the corresponding entries of the associated degrees of freedom.

4. NUMERICAL SIMULATION

4.1. COMPUTATIONAL ALGORITHM

By utilizing the constrained form of Lagrange's equations, the elastodynamic model of the multibody system can be written as

$$[\bar{M}]\{\ddot{\mathbf{q}}\} + [\bar{G}]\{\dot{\mathbf{q}}\} + [\bar{K}]\{\mathbf{q}\} + \{\bar{Q}\} + [J]^{\mathrm{T}}\{\lambda\} = \{\bar{F}\}, \tag{64}$$

where $[\bar{M}]$ is the non-linear inertia matrix for the coupled rigid and elastic degrees of freedom, global $[\bar{G}]$ is the gyroscopic damping matrix, $[\bar{K}]$ is the generalized stiffness matrix, $\{\bar{Q}\}$ is the quadratic velocity vector that includes the Coriolis and the gravitational force components, $[J]$ is the Jacobian matrix of the prismatic joint reference constraints and $\{\bar{F}\}$ is the external force vector. The generalized co-ordinate vector $\{\mathbf{q}\}$ is defined as

$$\{\mathbf{q}\} = [q_r^{\mathrm{T}}, q_e^{\mathrm{T}}]^{\mathrm{T}}, \tag{65}$$

where q_r is the vector of unconstrained rigid body degrees of freedom (three for the hub and three for the reference motion of the beam), and q_e is the vector of nodal degrees of freedom of the elastic beam.

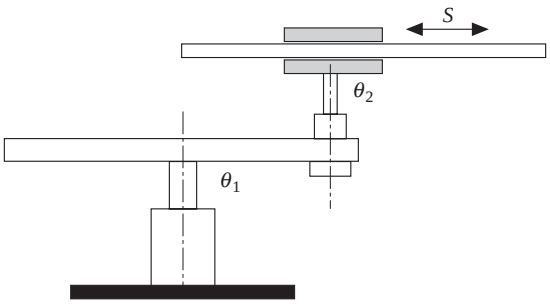

Figure 2. Schematic diagram of a planar mechanism.

Once the initial conditions are specified, static equilibrium analysis is performed to obtain the initial values of the elastic coordinates that are compatible with the assigned initial deflection shape. Then, equation (64) can be integrated forward in time by using integration algorithms similar to those of reference [30], and the system's time response thus can be predicted.

In this computational scheme, the effect of the prismatic joint constraints as imposed on the elastic beam is twofold. First is the effect on the beam reference motions by reducing them to one relative motion with respect to the rigid hub. This part is handled by the Jacobian matrix of the constraints on the multibody system. Second is the effect on the elastic deformations of the nodes that become enclosed by the hub. In practice the clearance between the contact surfaces within the prismatic joint is very small. Therefore, the elastic deformations of the enclosed nodes are eventually suppressed or reduced to vanishingly small values. In other words, the enclosed element will behave as a rigid element: i.e., one that has a reference motion with negligible local deformations.

The computational idea of the transition element is introduced to account for the aforementioned second effect of the prismatic joint constraints. The transition element is an element which is partially enclosed by the hub, and may have any numbering in the finite element configuration. One may add that there is no specific element called the transition element. However, at any given instant of time, one has three types of elements: namely, a type of element which is not at any contact with the prismatic joint hub (treated as a normal finite element), another type of element which is completely housed inside the hub (treated as a rigid element), and the third type which is in a transition stage: i.e., partially in contact with the hub (treated as a transitional finite element). If one considers the enclosed portion of the transition element to behave in a rigid manner then the remaining portion of the element will deform with a varying stiffness according to its changeable overhanging length outside the hub. Consequently, the contribution of the transition element to the flexibility of whole beam becomes a function of its unconstrained length (i.e., the portion of its length that extends outside the joint hub). For instance, in the case of retraction, the stiffness of the transition element increases as its unconstrained length decreases.

It is noteworthy to mention that the use of a multibody formulation of an interconnected system of rigid and flexible bodies has facilitated the computations of such a complicated problem. In this regard, the beam rigid-body or reference motion is accounted for by the inclusion of the rigid body generalized co-ordinates $\{q_r\}$. In addition, the full dimension of the elastic co-ordinates $\{q_e\}$ is also maintained throughout the formulation: that is, no elements are eliminated from the finite element mesh once they become enclosed by the rigid hub. In this case, the enormous numerical book-keeping which may be necessary with other variable length methods is no longer required.

TABLE 1

Flexible beam data

Property	Symbol	Value
Length (m)	L_t	3·6
Mass per unit length (kg/m)	ρ	4·015
Cross-section (mm)		152·4 × 9·52
Flexural rigidity (Nm^2)	EI	756·65

The numerical technique adopted in this scheme calls for freezing the elastic degrees of freedom of the enclosed nodes by filling out zeros in their corresponding entries for all coefficient matrices and ones for the corresponding diagonal entries of the mass matrix [31, 32]. In this case, the very small elastic deformations are approximated by zeros. The full dimension of the model is preserved, and no additional numerical book-keeping is necessary, since the nodal undeformed locations are known with respect to the local beam axis.

4.2. NUMERICAL EXAMPLES

In this numerical simulation, a planar arm with one prismatic and two revolute joints, shown in Figure 2, is considered. The assembly consists of a flexible link sliding through a rigid prismatic joint hub. The hub is attached by a revolute joint to a rigid shoulder which, in turn, is attached to the base by another revolute joint. The flexible link is a uniform slender beam similar to that used in reference [33]. The beam is made of aluminum with data shown in Table 1.

Hermitian shape functions are used to describe the Euler–Bernoulli finite beam element and the beam is discretized into four equal beam elements. The finite element mesh configuration of the elastic beam during deployment is shown in Figure 3. In this case, the numerical status of the transition element was assigned to any element which is partially enclosed by the hub during deployment. The detailed expressions for the elemental matrices and vectors can be found in reference [29].

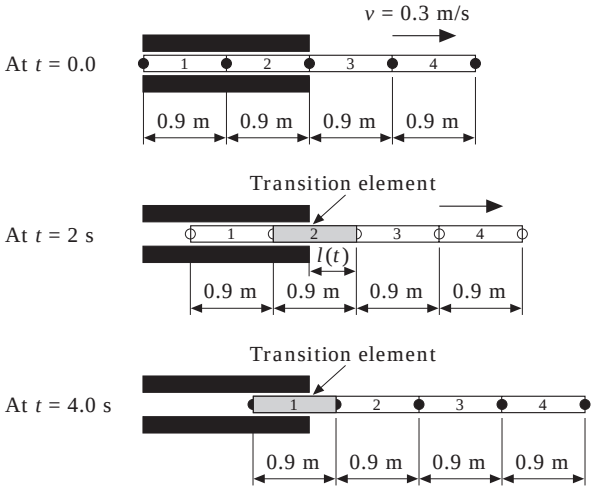

Figure 3. Extending beam at different points in time showing the transition element.

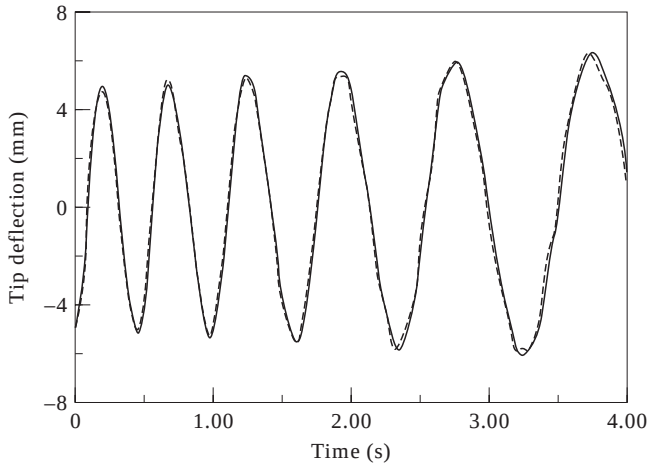

Figure 4. Tip deflection of a deploying beam; $v = 0{\cdot}3$ m/s. ——, AMM; · · · ·, FEM.

To simulate the case of an axially moving link, the motion of the hub is constrained such that no rotations are allowed. The flexible link with initial length of 1·8 m outside the hub of the prismatic joint is given an initial tip deflection of -5 mm. The link is then deployed at an axial velocity of 0·3 m/s and the tip deflections are compared with the results of the assumed modes solution [20] in Figure 4. Excellent agreement between the two methods is shown. The tip deflections of the retracting link from the initial length of 3 m outside the prismatic joint are compared with those given by the assumed modes solution in Figure 5. Figure 6 shows the effect of the end mass on the tip deflections of the deploying beam, where, as expected, the end mass reduces the frequency of oscillation and slightly increases the amplitude. It is noteworthy to mention that the assumed modes solutions of reference [20] were verified by using comparisons with the analytical solutions of references [7, 28] for both deployment and retraction of the beam motions. Excellent agreement between the results were reported in reference [28].

The case of axially moving link which is rotating about a fixed axis is simulated by preventing the rotation θ_1 of the shoulder revolute joint. The tip deflections of the axially moving and rotating link in the two cases of deployment and retraction are compared to

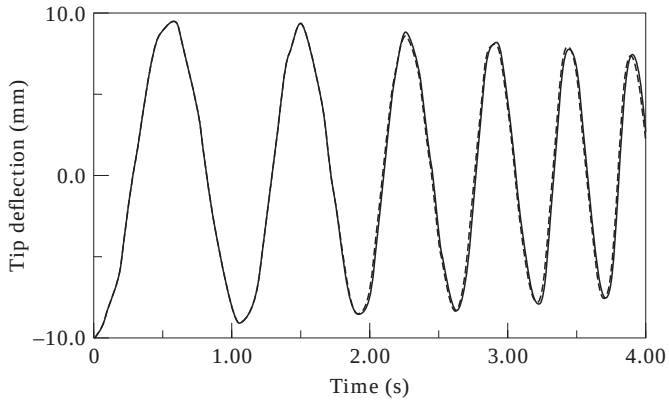

Figure 5. As Figure 4 but for retracting beam.

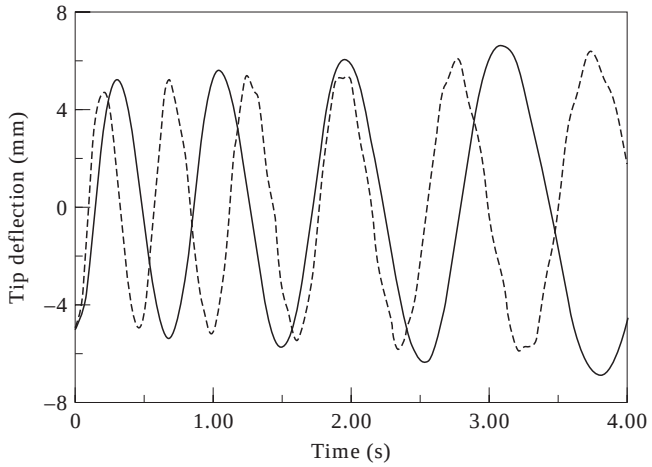

Figure 6. Tip deflection of a deploying beam; $v = 0{\cdot}3$ m/s. ——, with 2 kg end mass: · · · ·, without end mass.

the results of the assumed modes method in Figures 7 and 8, respectively. The comparison shows good agreement between the two solutions.

The capabilities of the model can now be explored by simulating the following two motion configurations: 1, a sliding link through a prismatic joint hub that executes curvilinear translation; 2, a sliding link through a prismatic joint hub that executes general planar motion.

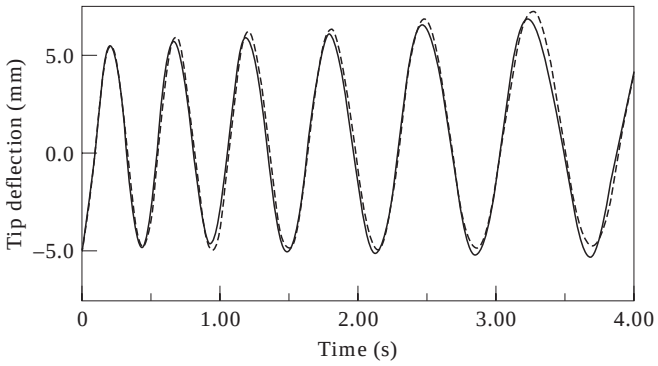

Figure 7. Tip deflection of a deploying and rotating beam; $v = 0{\cdot}3$ m/s and $w = 0{\cdot}1$ rad/s. ——, FEM; · · · ·, AMM.

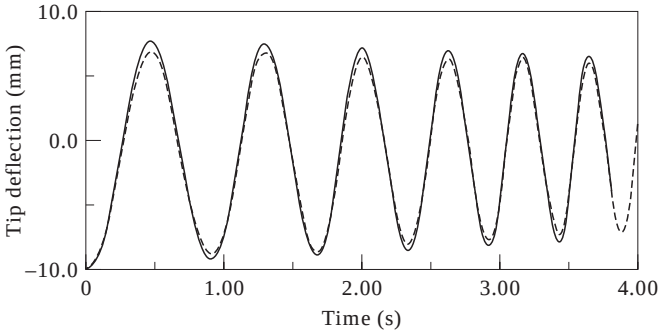

Figure 8. As Figure 7 but for retracting and rotating beam.

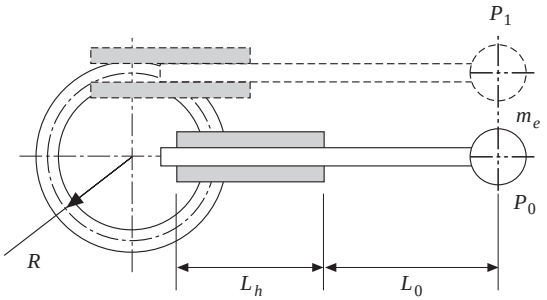

Figure 9. Planar configuration 1.

The first configuration, shown in Figure 9, is obtained by allowing rotation about both the base and the shoulder joints. In this simulation, the link deploys for 1 m, while the base joint is rotating an angle $\theta_1 = \pi/2$ and the shoulder joint is rotating an angle $\theta_2 = -\pi/2$, simultaneously in four seconds. The tip deflections of the link as it moves from position P_0 to position P_1 are shown in Figure 10 for the two cases with and without end mass. For the reverse motion from position P_1 to position P_0, the tip deflections are shown in Figure 11.

Finally, a general planar motion configuration as shown in Figure 12 is presented. In the simulation, the beam deploys 1 m, while the base and shoulder joints rotate through angles $\theta_1 = \pi/2$ and $\theta_2 = \pi/2$ in four seconds, respectively. The tip deflections for the forward motion from P_0 to P_2, and the reverse motion from P_2 to P_0 are displayed in Figures 13 and 14 respectively.

5. CONCLUSIONS

A finite element dynamic model of a sliding link through a prismatic joint where the prismatic joint hub is executing general planar motion is established. The model presents an attractive formulation which takes account of the general planar motion of the prismatic joint hub. All other reported models are confined to the case where the joint hub rotates about a fixed axis in space. Unlike in previous investigations, a finite element mesh with a fixed number of elements, is used where the element length is constant. The time-dependent boundary conditions manifested by the prismatic joint constraints are

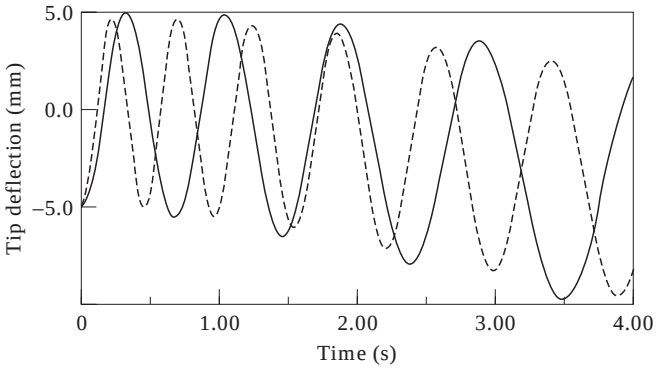

Figure 10. Tip deflection while moving from P_0 to P_1. ——, with 2 kg end mass; · · · ·, without end mass.

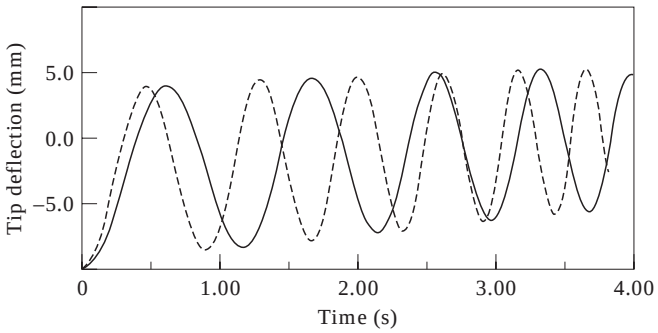

Figure 11. As Figure 10 but moving from P_1 to P_0.

considered. A transition element with variable stiffness is introduced at the interface with the joint hub. In this finite element formulation, all the inertia coupling terms between the beam reference motions and the local elastic deformations are considered. In addition, the model accounts for the dynamics of the end mass as well as the associated coupling effects.

The elastodynamic model developed in this paper is applicable to the general case of a flexible beam sliding relative to its rotating prismatic joint hub. In this formulation, the hub is treated as rigid. However, the hub dynamics is taken into consideration, where the general planar motion of the hub is accounted for. The elastic motion of the beam is represented by the small elastic deformations within the assumptions of linear theory of elasticity. The beam can either be kinematically driven or driven by a prescribed forcing functions.

The model offers the following advantages over the previously reported models that utilize a changeable finite element mesh.

1. The fixed nodal locations provide an attractive feature for control applications where point-sensors and point-actuators need to be placed at specified nodal points.

2. It eliminates the need for regenerating the coefficient matrices of the whole finite element model at each time-step. Here, only the stiffness matrix of a transition element is updated at each time-step.

3. It avoids the numerical difficulties associated with the continuity conditions when interfacing the displacements and velocities of the new nodes with the old ones. In this model, nodal points belong to an unchangeable finite element mesh.

4. It is more oriented to be integrated into a general dynamic analysis code.

The numerical simulations and comparisons with results of other methods have demonstrated the validity, accuracy and versatility of the developed scheme.

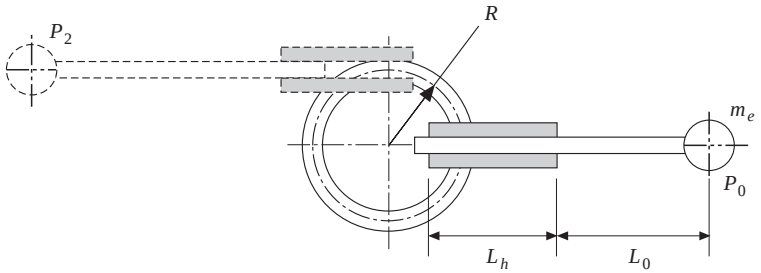

Figure 12. Planar configuration 2.

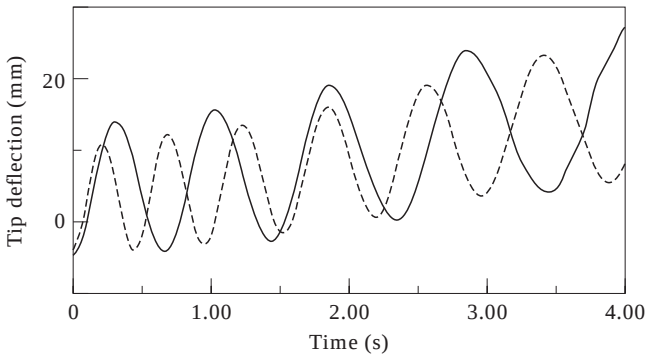

Figure 13. Tip deflection while moving from P_0 to P_2. ——, with 2 kg end mass; · · · ·, without end mass.

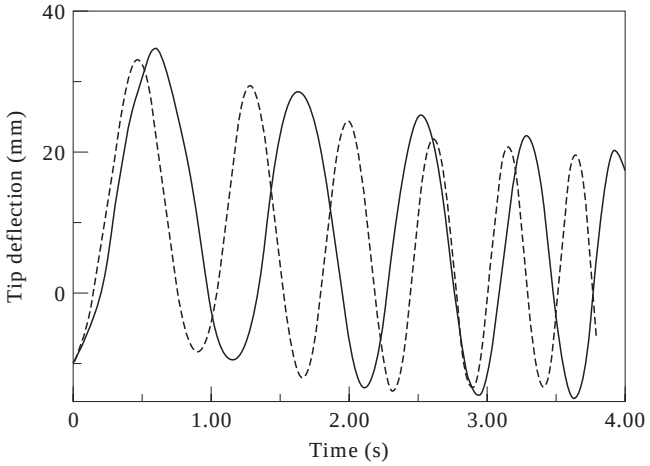

Figure 14. As Figure 13 but moving from P_2 to P_0.

ACKNOWLEDGMENT

The support of King Fahd University of Petroleum and Minerals is greatly appreciated.

REFERENCES

1. C. D. Mote 1965 *Journal of the Franklin Institute* **279**(6), 430–444. A study of band saw vibrations.
2. R. Barakat 1968 *Journal of the Acoustical Society of America* **43**(3), 533–539. Transverse vibrations of a moving thin rod.
3. B. Tabarrok, C. M. Leech and Y. I. Kim 1974 *Journal of the Franklin Institute* **297**, 481–494. On the dynamics of an axially moving beam.
4. K. W. Buffinton and T. R. Kane 1985 *International Journal of Solids and Structures* **21**, 617–643. Dynamics of a beam moving over supports.
5. P. K. C. Wang and J. D. Wei 1987 *Journal of Sound and Vibration* **116**, 149–160. Vibrations in a moving flexible robot arm.

6. G. E. Weeks 1986 *Journal of Spacecraft* **23**, 102–107. Dynamic analysis of a deployable space structure.
7. S. Kalaycioglu and A. K. Misra 1991 *Journal of Guidance* **14**, 287–293. Approximate solutions for vibrations of deploying appendages.
8. K. Tsuchiya 1983 *Journal of Guidance* **6**, 100–103. Dynamics of spacecraft during extension of flexible appendages.
9. V. J. Modi and A. M. Ibrahim 1984 *Journal of Guidance* **7**, 563–569. A general formulation for liberational dynamics of spacecraft with deploying appendages.
10. A. G. Ulsoy and C. D. Mote 1982 *Journal of Engineering for Industry* **104**, 71–78. Vibration of wide band saw blades.
11. C. D. Mote and J. A. Wickert 1988 *Journal of the Acoustical Society of America* **84**, 963–969. Linear transverse vibration of an axially moving string particle systems.
12. S. T. Ariaratnam and S. F. Asokanthan 1993 *Journal of Sound and Vibration* **167**, 421–432. Instabilities in moving bands under random tension fluctuation.
13. J. A. Wickert 1993 *Journal of Sound and Vibration* **160**, 455–463. Analysis of self excited longitudinal vibration of a moving tape.
14. J. A. Wickert and C. D. Mote 1988 *Shock and Vibration Digest* **20**(5), 3–13. Current research on the vibration and stability of axially moving materials.
15. N. G. Chalhoub and A. G. Ulsoy 1986 *Journal of Dynamic Systems, Measurement and Control* **108**, 119–126. Dynamic simulation of lead screw driven flexible robot arm and controller.
16. P. K. C. Wang and J. D. Wei 1987 *Proceedings of the IEEE International Conference on Robotics and Automation* 1683–1689. Feedback control of a moving flexible arm with rotary and prismatic joints.
17. K. Krishnamurthy 1989 *Journal of Sound and Vibration* **132**, 143–154. Dynamic modeling of a flexible cylindrical manipulator.
18. J. Yuh and T. Young 1991 *Journal of Dynamic Systems, Measurement and Control* **113**, 34–40. Dynamic modeling of an axially moving beam in rotation: simulation and experiment.
19. K. W. Buffinton 1992 *Journal of Dynamic Systems, Measurement and Control* **114**, 41–49. Dynamics of elastic manipulators with prismatic joints.
20. B. O. Al-Bedoor and Y. A. Khulief *Journal of Sound and Vibration* **190**, 195–206. Vibrational motion of an elastic beam with prismatic and revolute joints.
21. A. K. Banerjee and T. R. Kane 1989 *Journal of Guidance, Control and Dynamics* **12**, 140–146. Extrusion of a beam from a rotating base.
22. Y. C. Pan, R. A. Scott and A. G. Ulsoy 1990 *Journal of Mechanical Design* **112**, 307–314. Dynamic modeling and simulation of flexible robots with prismatic joints.
23. F. Gordaninejad, A. Azhdari and N. G. Chalhoub 1991 *Journal of Vibration and Acoustics* **113**, 461–468. Nonlinear dynamic modeling of a revolute-prismatic flexible composite-material robot arm.
24. Y. K. Kim and J. S. Gibson 1991 *IEEE Transactions on Robotics and Automation* **7**, 818–827. A variable-order adaptive controller for a manipulator with a sliding flexible link.
25. J. D. Downer and K. C. Park 1993 *AIAA Journal* **31**, 339–347. Formulation and solution of inverse spaghetti problem: application to beam deployment dynamics.
26. M. Stylianou and B. Tabarrok 1994 *Journal of Sound and Vibration* **178**, 433–453. Finite element analysis of an axially moving beam, Part I: Time integration.
27. L. Vu-Quoc and S. Li 1995 *Computer Methods in Applied Mechanics and Engineering* **120**, 65–118. Dynamics of sliding geometrically-exact beams: large angle maneuver and parametric resonance.
28. B. O. Al-Bedoor and Y. A. Khulief 1996 *Journal of Sound and Vibration* **192**, 159–171. Approximate analytical solution of beam vibrations during axial motion.
29. B. O. Al-Bedoor and Y. A. Khulief 1996 *Computer Methods in Applied Mechanics and Engineering* **131**, 173–189. Finite element dynamic modeling of a translating and rotating flexible link.
30. L. F. Shampine and M. K. Gordon 1975 *Computer solution of ordinary differential equations: The initial value problem*. W. H. Freeman.
31. R. D. Cook 1981 *Concepts and applications of finite element analysis* (second edition) New York: John Wiley.
32. D. R. J. Owen and E. Hinton 1980 *Finite element in plasticity: theory and practice*. Pineridge Press.
33. S. S. Tadikonda and H. Baruh 1992 *Journal of Dynamic Systems, Measurement and Control* **114**, 422–427. Dynamics and control of a translating beam with prismatic joint.

APPENDIX: NOMENCLATURE

A Rotational transformation matrix.
A_θ Derivative of the transformation matrix.
C Gyroscopic matrix.
EI Flexural rigidity.
F_S Axial external force.
F_θ Rotational external force.
F_q Nodal external forces.
F_X external force in X-direction.
F_Y external force in Y-direction.
G Gyroscopic matrix.
K Strain stiffness matrix.
k_{qq} Generalized stiffness matrix.
k_a Rotational stiffness matrix.
L Lagrangian function.
L_h Hub length.
l Finite element length.
m_{qq} Consistent mass matrix.
m_{Sq} Inertial coupling vector.
m_{SS} Axial inertia.
$m_{\theta\theta}$ Rotational inertia.
m_{XX} X-translational inertia.
m_{YY} Y-translational inertia.
m_e End mass.
N Shape functions.
n Number of finite elements.
Q nonlinear force vector.
q_e Vector of nodal degrees of freedom.
q_r Vector of reference degrees of freedom.
R Position vector in the inertial frame.
S_i The axial location of node i.
U Kinetic energy.
u Elastic displacement.
V Potential energy.
XY Inertial reference frame.
xy Body fixed axes.
$x^i y^i$ Element co-ordinate system.
ρ Mass per unit length.
δ Axial shortening due to bending deformations.